STATUS REPORT FOR NAG 5 1578
Period: 5/91-12/91

Gamma-Ray Spectroscopy: The Diffuse Galactic Glow

D. Hartmann(PI)
Department of Physics and Astronomy
Clemson University

ABSTRACT

The goal of this project is the development of a numerical code that provides statistical models of the sky distribution of gamma-ray lines due to the production of radioactive isotopes by ongoing Galactic nucleosynthesis. We are particularly interested in quasi-steady emission from novae, supernovae, and stellar winds, but continuum radiation and transient sources must also be considered. We have made significant progress during the first half period of this project and expect the timely completion of a code that can be applied to OSSE Galactic plane survey data.

REPORT

a) Nucleosynthesis

For the nuclear species considered in this study, the so-called α-process is of particular interest. CO-I Woosley and his graduate student R. Hoffman have carrried out extensive simulations of parametrized explosive synthesis for material that is initially in nuclear statistical equilibrium and is cooled so rapidly that the freeze-out from equilibrium occurs in the presence of a large helium abundance. The physics of this α-process and the resulting nuclear yields is described in Woosley and Hoffman (1992). The particular aspects of ^{44}Ti are discussed in Woosley and Hoffman (1991). The results of these recent nucleosynthesis studies (and other not mentioned here) have been incorporated in the code under development.

b) Galactic Models

The current status of the code includes only smooth Galactic features (spiral arms etc will be included later), and we have sofar only included supernovae in the simulation. Spatial distributions and rates of supernovae of various kinds have been obtained from recent extra-galactic surveys. We have included a dust extinction model of the Galaxy to simulate the historic supernova rate in order to constrain model parameters. Nuclear yields have been provided by CO-I Woosley. We have used this code to constrain the Galactic supernova rate from the absence of gamma-ray line emission due to the decay of ^{44}Ti. The code in its current state is already superior to that employed by Mahoney etal. (1990) for a similar study. The results of this test application have been presented at the 2nd GRO Science Workshop (Hartmann etal. 1991) and a more detailed paper is in preparation for

c) Photon Sky Maps

Ultimately, we will use the predicted gamma-ray fluxes from the superposition of many Galactic sources to model the integrated photon flux on the sky. To become familiar with the data analysis and interpretation needs for this step, we have installed the COS-B database on Clemson workstations and developed the data IO and image analysis software necessary to work with this database. Our approach is based on a smooth photon probability map rather than a direct photon count map. This is motivated by the natural smearing of photon arrival directions by gamma-ray detectors. We hope to be able to employ our techniques in conjunction with the OSSE plane survey and the presentation/analysis of the simulated maps produced by our code. As a by-product of this work, we have found a way to enhance the signal-to-noise ratio in searches for pulsating gamma-ray sources superimposed on a strong background. The results of this aspect of our diffuse glow project were presented at the 2nd GRO Science Workshop (Brown, Clayton, and Hartmann 1991).

d) Transient Sources

In addition to research directly aimed at developing the gamma-ray mapping code for line emission from ongoing nucleosynthesis, grant NAG 5 1578 also provided partial support for the PI's research on transient Galactic gamma-ray emission. In collaboration with Dr. David Band at UCSD, the PI investigated the effect of ionizing radiation from burst sources on their environment. The results of this study were presented at the Huntsville gamma-ray burst workshop and a paper was accepted for publication in ApJ (Band and Hartmann 1991, 1992). In collaboration with Dr. Boyd (Ohio State University) Galactic continuum and line emission induced by transient gamma-ray emission was investigated. Possible secondary signals arising from interactions of primary photons from a burster with surrounding material can result from pair annihilation or from the decay of unstable nuclei that were created by the photoerosion process. The results of this work were presented at the Huntsville burst workshop and an ApJ paper on this subject is in preparation (Fencl, Boyd, and Hartmann 1991, 1992). Whether gamma-ray bursts are associated with Galactic neutron stars has become another Great Debate. The Clemson group has carried out statistical studies involving Galactic neutron stars and also calculated more general geometric models, as well as cosmological models. The findings of this work were reported at the Huntsville workshop (Hartmann etal 1991) and a paper suggesting that bursts come from Pop II neutron stars in the Galactic halo has been submitted to Nature (Hartmann 1991). In light of the recent BATSE results, perhaps only some bursts are associated with neutron stars, evidenced by their cyclotron lines and other circumstantial evidence. In that case, bursts may be due to glitches in the neutron star rotation. We have placed an upper limit on the energy conversion efficiency of such models from observations with Phobos detectors (Hartmann, Hurley, and Niel 1992). The debate on the distance to gamma-ray bursts depends to a large extent on the interpretation of the BATSE finding of an isotropic sky distribution together with an inhomogenous space distribution as measured by the V/V_{max} test. In collaboration with Hurley (UCB) and Gonzalez (UCSC) a refined analysis tool was developed that takes counting noise errors into account (Hartmann, Gonzalez, and Hurley 1991).

e) Future Work

We have completed the development of the basic framework for the code and have demonstrated its current use with a study of the Galactic emission from ^{44}Ti (Hartmann etal. 1991). We are now including more isotopes, more specific sources (novae, WR and AGB stars), and the effects of spiral structure. We need to develop more graphical presentation tools for the photon sky maps. Clemson graduate student S. Guha has become involved in all aspects of our diffuse glow project and is expected to contribute greatly to the development of this tool. Under NRA 91-OSSA-22 the grant team has submitted a GRO Phase II "renewal" proposal for this project and in collaboration with Dr. M. Leising (Clemson) the PI has also submitted a specific observing proposal to OSSE aimed at determining the importance of spiral arm "fine structure" that we plan to model with the next version of the code. To improve further our nucleosynthesis prescriptions for WR stars we will collaborate with Dr. M. F. El Eid (Goettingen Observatory, FRG), who will spend the spring 1992 semester at Clemson.

REFERENCES

"Flash-photoionization of gamma-ray burst environments", Band, D. L., and Hartmann, D. H. 1992, ApJ, Feb. 10 issue, in press

"Gamma-ray bursts and radio pulsar glitches", Hartmann, D., Hurley, K., and Niel, M. 1992, ApJ, in press

"A modified V/Vmax test for gamma-ray bursts", Hartmann, D., Gonzalez, J. J., and Hurley, K. 1991, ApJ, submitted

Gamma-Ray Pulsar analysis from photon probability maps, 2nd GRO workshop Brown, L., Clayton, D. D., & Hartmann, D. 1991, in press

Gamma-Ray constraints on the Galactic supernova rate, Hartmann, D., The, L.-S., Clayton, D. D., Leising, M., Mathews, G., and Woosley, S. E. 1991, 2nd GRO workshop, in press

Cosmic gamma-ray bursts from BATSE: Another great debate, Hartmann, D, The, L-S., Clayton, D. D., Schnepf, N. G., & Linder, E. V. 1991, Huntsville, submitted

The ionization of gamma-ray burst environments, Band, D., and Hartmann, D. 1991, Huntsville workshop, in press

Gamma-ray line afterglow from burst environments, Fencl, H., Boyd, D., & Hartmann, D. 1991, Huntsville, in press

Gamma-ray line afterglow from burst environments, Fencl, H. S., Boyd, R. N., and Hartmann, D. 1992, ApJ, in preparation

^{57}Co and ^{44}Ti production in SN1987A, Woosley, S. E., and Hoffman, R. 1991, ApJL, 368, L31

The α-process and the r-process, Woosley, S. E., and Hoffman, R. 1992, ApJ, in press

HEAO 3 limits on the ^{44}Ti yield in Type I supernovae, Mahoney, W. A., Ling, J. C., Wheaton, W. A., and Higdon, J. C. 1990, in *Gamma-Ray Line Astrophysics*, AIP 232, 291

Gamma-ray bursts from old Pop II neutron stars in the Galactic halo, Hartmann, D. 1992, Nature, submitted

Appendices

To assist in this grant performance review, we include copies of the two papers most closely related to the goal of this study: (Brown, Clayton, and Hartmann 1991; Hartmann etal. 1991).

Gamma-Ray Constraints on the Galactic Supernova Rate

D. Hartmann, L.-S. The, D. D. Clayton, M. Leising,
Department of Physics and Astronomy
Clemson University, Clemson, SC 29634
and
G. Mathews
Department of Physics
Lawrence Livermore National Laboratory
Livermore, CA 94551
and
S. E. Woosley
Board of Studies in Astronomy and Astrophysics
UCO/Lick Observatory, University of California
UCSC, Santa Cruz, CA 95064

Abstract

Most Galactic supernovae are hidden from our view due to severe extinction in the Galactic plane. In the γ-ray band the Galaxy is almost transparent so that we could detect supernovae that are obscured. ^{44}Ti is among the potentially detectable isotopes in supernova ejecta. Surveys carried out with the HEAO 3 experiment and γ-ray detectors aboard the Solar Maximum Mission (SMM) have not detected γ-ray lines expected from the decay chain $^{44}\mathrm{Ti} \rightarrow {}^{44}\mathrm{Sc} \rightarrow {}^{44}\mathrm{Ca}$. These observations thus constrain the rates and nucleosynthesis of supernovae. We perform Monte Carlo simulations of the expected γ-ray signatures of Galactic supernovae of all types to estimate the significance of the lack of a γ-ray signal due to supernovae occuring during the last millenium. Using recent estimates of the nuclear yields we determine mean Galactic supernova rates consistent with the historic supernova record and the γ-ray limits. Another objective of these calculations of Galactic supernova histories is their application to surveys of diffuse Galactic γ-ray line emission.

1 Introduction

Detection of γ-ray line emission from ongoing Galactic nucleosynthesis is one of the major observational goals of γ-ray astronomy. We consider the signal from the decay $^{44}\mathrm{Ti} \rightarrow {}^{44}\mathrm{Sc} \rightarrow {}^{44}\mathrm{Ca}$. Measurements of the ^{44}Ti half-life prior to 1965 implied $t_{1/2} \leq 50$ years, but recent Brookhaven measurements suggest a much longer half-life of 66.6 years (Adelberger & Harbottle 1990). Here we adopt the intermediate half-life of 54.2 years (Frekers *et al.* 1983), corresponding to $\tau = 78.2$ years, which was also employed by Mahoney *et al.* (1991). Pinning down the correct value remains an important objective in nuclear astrophysics. Because of this short life-time, detection of a γ-ray signal from ^{44}Ti involves either very recent or very near supernovae.

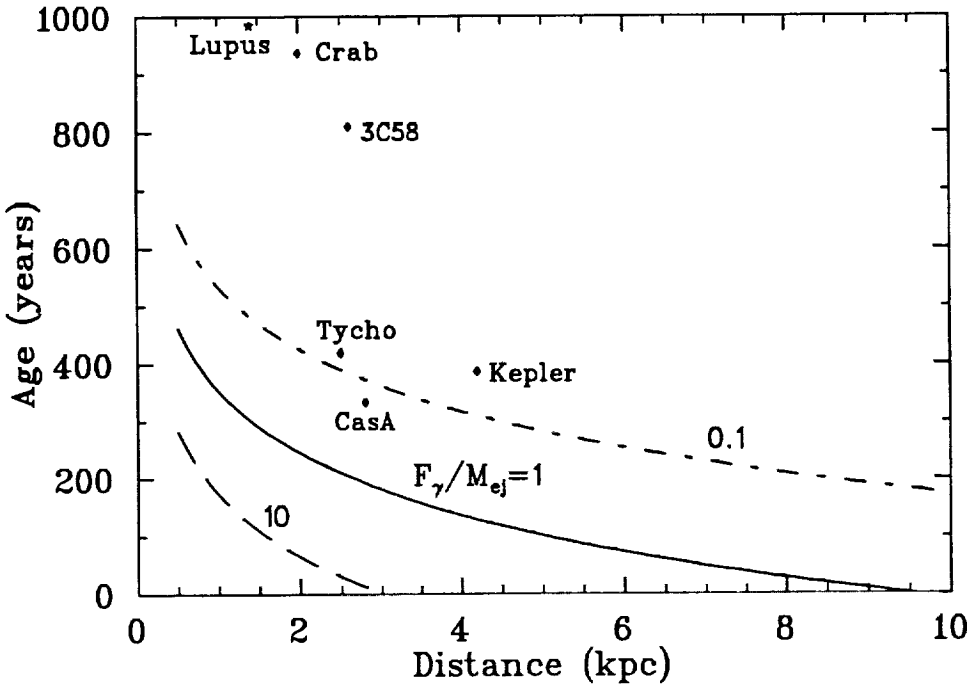

Figure 1: *Age distance relationship for γ-ray line emission from ^{44}Ti. Source detectability depends on the ratio of flux limit to ejected mass, F_γ/M_{ej}. Six historic supernovae are shown.*

The decay of ^{44}Ti generates three γ-ray photons with energies of 78.4 keV, 67.9 keV, and 1.157 MeV. The resulting line flux at earth is

$$F_\gamma \sim 1 \times 10^{-2}\ M_{-4}\ \exp(-t/78.2\ \mathrm{yrs})\ D^{-2}(kpc)\ \ \mathrm{photons\ cm^{-2}s^{-1}}\ ,$$

where M_{-4} is the ejected ^{44}Ti mass in units of 10^{-4} $M_\odot$ The detectability of such emission from recent supernovae in our Galaxy and perhaps from a few older but nearby remnants make this nucleus a prime γ-ray target (Figure 1). It is clear, however, that the search for ^{44}Ti line emission from previously undetected Galactic supernovae deals with the few events of the past couple of centuries, so that the interpretation of line detection, or lack thereof, is statistical in nature. This is similar to the situation of ^{22}Na, and our Monte Carlo analysis is conducted in the spirit of Higdon and Fowler's (1987) analysis of ^{22}Na detectability from novae.

Searches for ^{44}Ti line emission have been carried out using the high-resolution γ-ray spectroscopy experiment on HEAO 3 (Mahoney *et al.* 1991) and the γ-ray spectrometer aboard the SMM satellite (Leising & Share 1991). No signal was detected with either instrument. Mahoney *et al.* (1991) used the HEAO 3 limit to constrain the combination of supernova rate and mass of ^{44}Ti ejected per event, but considered the relevant supernovae to be of Type Ia and ignored constraints from the optical signature of these events. Current nucleosynthesis estimates for ^{44}Ti suggest that in fact supernovae involving massive stars (Type Ib and II) may dominate the production of this isotope. We take a somewhat different approach and utilize current yield estimates (and their uncertainties) to constrain exclusively the mean Galactic supernova rate.

2 Yields and Sites

To achieve full solar production of ^{57}Fe and ^{44}Ca their γ-ray emitting progenitors ^{57}Ni and ^{44}Ti must be produced in environments that guarantee a significant contribution from the so called "alpha-rich freeze-out" (Woosley, Arnett, & Clayton 1973). This component can be expected when low density matter falls out of nuclear statistical equilibrium (NSE) while being cooled so rapidly that free alpha particles have insufficient time to reassemble back into more massive nuclei. In contrast to normal freezeout from NSE at high densities, the large mass fraction of surviving alpha particles drastically alters the resulting nucleosynthesis. It is generally believed that alpha-rich freeze-out must be invoked to explain solar abundances of several isotopes, including ^{57}Fe, ^{59}Co, ^{58,60,61,62}Ni, and ^{64}Zn (Woosley 1986). We utilize the fact that the synthesis of ^{44}Ti and ^{57}Ni occurs in similar, if not the same, astrophysical sites, and take advantage of observations of SN 1987A to estimate ^{44}Ti yields. Mahoney *et al.* (1991) treated the titanium yield as a free parameter and assumed it to be the same for all events.

The bolometric luminosity of SN 1987A at late times is dominated by the radioactivity of ^{44}Ti (e.g., Woosley, Pinto, & Hartmann 1989). The abundance of ^{44}Ti is sensitive to pre-explosive details of stellar evolution as well as the explosion mechanism. For SN 1987A Kumagai *et al.* (1989) and Woosley & Pinto (1988) estimate Ti production near 10^{-4} $M_\odot$. This result is uncertain by at least a factor of two. Parametrized nucleosynthesis studies (Woosley & Hoffman 1991: WH) can also be used to constrain production of ^{44}Ti. Assuming that ^{56}Ni is the dominant constituent of iron group elements ejected in SNII and using a conservative lower limit on the neutron enrichment parameter $\eta \lesssim 10^{-3}$, the parametrized synthesis calculations constrain the ratio $r_{57} = X(^{57}Ni)/X(^{56}Ni)$. To avoid overproduction of ^{58}Ni by a factor of 5 or more, WH finds $r_{57} \lesssim 2 r_{57\odot}$. The lower limit on η corresponds to a lower limit $r_{57} \gtrsim 0.3$ $r_{57\odot}$ in the case that an α-rich freeze-out does not occur. For the most realistic η values and a modest α-rich freeze-out WH find $r_{57} \gtrsim 0.7\ r_{57\odot}$.

Production of ^{44}Ti and ^{57}Co is dominated by stellar zones that have experienced some alpha-rich freeze-out. Thus, the limits on ^{57}Co also provide a constraint on the ^{44}Ti yields. WH find that a Ti production ratio $P_{44} = {}^{44}Ti/{}^{56}Fe$ close to solar ($P_{44\odot} \sim 1.2\times10^{-3}$) occurs for a variety of conditions and that the upper limit on r_{57} restricts P_{44} to less than twice solar. Recent observations of the bolometric light curve of SN 1987A suggest $r_{57} \sim 5$ (Suntzeff *et al.* 1991), which implies copious co-production of ^{44}Ti ($P_{44} \sim 2P_{44\odot}$) in Type II supernovae, but the uncertainties in modeling the bolometric lightcurve are still very large. Dynamic simulations of explosive nucleosynthesis (Hashimoto *et al.* 1989; Kumagai *et al.* 1989; Woosley, Pinto, & Weaver 1988; Woosley 1991) estimate $P_{44} \sim 1.5\text{–}2.5\ P_{44\odot}$, so that a typical Type II supernova might eject $10^{-4} M_\odot$. However, these simulations are not yet realistic, because they assume either a piston or instantaneous energy deposition. We randomly select the ejected ^{44}Ti mass in SNII from $M_{ej} \sim \zeta\ P_{44\odot}\ M_{56}$, where ζ is randomly chosen between 0.5 and 2.0, and the ejected mass of ^{56}Fe varies between $2\times10^{-3} M_\odot$ and 0.3 $M_\odot$ for stars with initial mass between 10 $M_\odot$ and 35 $M_\odot$. The initial mass was selected from a Salpeter IMF by another random number. The same prescription is used for SNIb, but the amount of ejected ^{56}Fe is kept fixed at 0.3 $M_\odot$, because not enough SNIb have been observed to estimate their intrinsic spread in iron production. For SNIa we randomly draw an ejected iron mass between 0.25 $M_\odot$ and 0.75 $M_\odot$, and select ζ between 0.03 and 0.08. The titanium synthesis in these exploding carbon-oxygen white dwarfs is not very well known, but recent models of delayed detonations (DD) support

the ζ range employed here. In DD models of Type Ia supernovae substantial production of intermediate mass isotopes (O, Mg, Si, Ca..) occurs because the detonation wave propagates through low density matter in the pre-expanded white dwarf envelope. Estimates of the yields of isotopes in this mass range are sensitive to the uncertain transition density where the initial deflagration turns into a detonation.

The rate of SNIa is about a factor 10 smaller than that of supernovae involving massive stars (Ib & II). Thus, the Galactic nucleosynthesis of ^{44}Ti could be dominated by SNII and SNIb, but from the point of view of γ-ray searches for individual Galactic events only the product $\zeta P_{44\odot}$ M_{56} matters. Although uncertain, the values discussed above clearly indicate that one must include all supernova classes in the analysis.

3 Event Distribution

3.1 Spatial Distributions

The standard scenarios for Type Ia supernovae involve accreting white dwarfs, which motivates the use of distribution models derived for novae (Higdon & Fowler 1987; Mahoney *et al.* 1991). The Galactic nova distribution is not well known because of severe extinction corrections. To alleviate this problem one relies on nova surveys of M31 where sample completeness is much higher (e.g., Ciardullo *et al.* 1987). From these observations one expects contributions from two distinct populations: disk and spheroid. We follow Higdon & Fowler (1987) who generate Monte Carlo representations of these populations from integral probability distributions for an axissymmetric disk and a spherically symmetric bulge component. The observations of M31 seem to suggest that the nova rate traces the blue light distribution. Using the Bahcall-Soneira Galaxy model Mahoney *et al.* (1991) argue that the fraction of SNIa occuring in the spheroid is about 1/6. The remaining two classes of events are thought to be associated with massive stars and thus follow a Pop I spatial distribution. We assume that birth places are exponentially distributed in height above the plane with a scale length of 100 pc. Ignoring spiral structure we assume smooth radial birth functions that are either constant within some radius σ_r, fall off exponentially with distance from the Galactic center (with scale length σ_r), or are ring-like $\rho(r) \propto \exp\left((r - r_0)^2/\sigma_r^2\right)$, where H_2 observations suggest that $r_0 \sim 5$ kpc.

3.2 Supernova Rates

Instead of treating the total Galactic rate of each supernova class as a free parameter, we fix the relative rates based on observations of external galaxies and vary the total rate. Relative supernova rates are sensitive to the type of the host galaxy (e.g., Tammann 1991). The Hubble type of the Milky Way is not accurately known, but is most likely between Sbc and Sd, so that the observations suggest the following breakdown (Ia:Ib:II) = (1:1.6:8) (Tammann 1991). We thus assume that a fraction $F_{Ia} \sim 0.09$ of all events is of type Ia. Similarly, the fraction of type Ib events among supernovae involving massive stars is $F_{Ib} \sim 0.16$. These values are used to randomly assign an event class.

4 Optical Constraints

4.1 The Historic Record

Supernovae are rare events in our Galaxy, only six are known to have occured during the last millenium. Without doubt, additional supernovae occured during that period but were not observed because of obscuration by interstellar matter. Still, we can use these historic events to constrain the range of acceptable mean Galactic supernova rates. Classification and peak magnitudes of historic events are uncertain, but we follow van den Bergh (1990) for the breakdown (Ia:Ib:II) $\sim$ (1:2:3). All of these events were brighter than $m_V = 0$. We assume that the historic record is complete above this level. On the other hand, the record of historic nova discoveries above the same limit suggests a rather strong time dependence, suggesting that the historic supernova record could be very incomplete as well (van den Bergh & Tammann 1991; van den Bergh 1991b; Tammann 1991). We allow for a factor 2 in all of the above numbers, so that there could have been a total of 12 detectable events.

Within about 4 kpc of the sun there were between 3 and 4 core collapse supernovae. From a comparison of the total Galactic Pop I content to that within a cylinder of that radius Ratnatunga and van den Bergh (1989) infer that the total Galactic core collapse rate is of order 6-8 events per century. This value is well above theoretical estimates based on integrating a reasonable IMF (van den Bergh 1991a) or values derived from extragalactic evidence (Evans, van den Bergh & McClure 1989) that give $\sim 2.2 \pm 2$ and 2.6 ± 0.7, respectively. This problem of an unexpectedly high apparent frequency of nearby supernovae has been discussed in detail by van den Bergh (1990). A supernova rate as high as 1/10 yrs requires a star formation rate that exhausts the available gas supply in the Galactic annulus of the solar neighborhood in less than $\sim 10^9$ yrs (van den Bergh 1991b). This is inconsistent with age estimates of the Galactic disk ($T_d \sim 10^{10}$ yrs) derived from white dwarf luminosity functions. We consider the possibility that the actual mean supernova rate is in fact as low as indicated by extragalactic observations and that the observed large number of local supernovae during the past millenium is just a statistical fluctuation.

4.2 Peak Magnitudes

Observations suggest that the absolute magnitude in the B-band for Type Ia supernovae is so well defined that we can use SNIa as standard candles (e.g., Leibundgut 1991; Branch & Tammann 1991). We follow Leibundgut and Tammann (1990) by employing $M_B(max) = -18.3 + 5\ log(h)$, where h is the Hubble constant normalized to 100 km/s/Mpc. Furthermore, the observations suggest that B-V $\sim$ 0 at maximum light. Throughout this paper we assume h=1. Supernovae of Type Ib are fainter than SNIa (e.g., Porter and Filipenko 1987). Because of its recent establishment as an independent class, too few events have been studied well enough to determine accurately their peak magnitude and intrinsic spread. We therefore assume a single value (Evans, van den Bergh, & McClure 1989) $M_B(max) = -16.7 + 5\ log(h)$. Still fainter at peak than SNIb's are Type II supernovae. We follow Tammann & Schröder (1990) and use $M_B(max) = -15.7 + 5\ log(h)$. To include the possibility of underluminous SNII, such as 1987A, we add uniform random fluctuations with amplitude $\delta M_B = 1.2$ mag. Tammann & Schröder (1990) use a Gaussian distribution that rarely gives such underluminous events, although these events could be common (e.g., Branch 1990; Schmitz & Gaskell 1988).

4.3 Extinction

Galaxy counts and photometric studies of stellar reddening at high Galactic latitudes imply a polar photographic extinction A_{ph} of about 0.25 mag or less than 0.1 mag, respectively (Heiles 1976; Burstein & McDonald 1975). However, a careful re-analysis of galaxy counts (Burstein & Heiles 1978) has shown that these data are too noisy to distinguish between zero extinction and a csc(b) law with an amplitude of 0.25 mag. The study by Burstein and Heiles also showed that a smooth csc(b) law does not give a good representation of extinction because of the patchiness in the interstellar dust component.

From the more reliable photometric studies of stars and globular clusters it appears that the extinction toward the galactic poles is of order of 0.2 mag or less. An extinction of 1 mag corresponds roughly to a hydrogen column density along the line of sight of N(HI) = 10^{21} cm^{-2} (Burstein and Heiles 1978). Extinction and optical depth, τ, at some wavelength are related by $A_\lambda = 1.086\ \tau_\lambda$. Although there still is considerable debate about the correct value of the polar extinction, the average optical depth of the half disk in spiral galaxies is commonly assumed to be of order $\tau_p = 0.2$ (e.g., Sandage and Tammann 1981). However, the question whether galaxy disks are optically thin or opaque is still debated (e.g., Disney, Davies, and Phillips 1989; Valentijn 1990). Because the radial scale length of the Galaxy is so much larger than the vertical scale height of the dust layer (which produces the bulk of the extinction) a total optical depth to the Galactic center may be as high as $\tau_c \sim 40$. In the solar neighborhood the average extinction per unit length is of order $\tau_a = 1$ kpc^{-1} (Mihalas and Binney 1981).

We employ simple extinction models that assume either constant, exponentially decaying, or ring-like density distributions with respect to galactocentric radius and that are either constant, exponentially decaying, or Gaussian with respect to the height above the Galactic plane. We normalize the resulting density distribution such that the polar optical depth is exactly equal to $\tau_p = 0.2$. To determine the extinction correction for a particular event in the Galaxy we first integrate along the line of sight and then add a maximally 50% correction, reflecting the patchiness of the ISM, by $\tau_{eff} = \tau(D)\ (1 - (r - 1/2)\exp(-\tau(D))$, where r is a uniform random variable between 0 and 1. The exponential factor reduces the fluctuations for observations of objects with large intervening column depths. After applying extinction corrections we consider a supernova optically detected when its apparent magnitude is brighter than m_v=0.

4.4 Results and Conclusions

Because of the short life time of ^{44}Ti the γ-ray glow of our Galaxy is expected to be dominated by perhaps a few recent events. However, as Figure 1 shows, none of the known historic supernovae is either close or young (or both) enough to be detectable in the "titanium window" (assuming standard yields). Thus one searches for emission from recent supernovae that remained unrecognized due to either Galactic absorption or gaps in sky coverage during the past millenium.

Mahoney *et al.* (1991) searched through the scan-by-scan data of the HEAO 3 γ-ray experiment. Of the three γ-ray lines associated with the decay of ^{44}Ti emission at 68.9 keV and 78.4 keV is most easily detectable by the HEAO 3 spectrometer. Mahoney *et al.* (1991) searched for flux enhancements in 16 channels covering the energy range 58–90 keV. The high-resolution spectrometer aboard HEAO 3 scanned the sky with a field of view of $\sim 30°$ and a period of about 20 minutes. Mahoney *et al.* (1991) analyzed the scans, searching for a point source at a

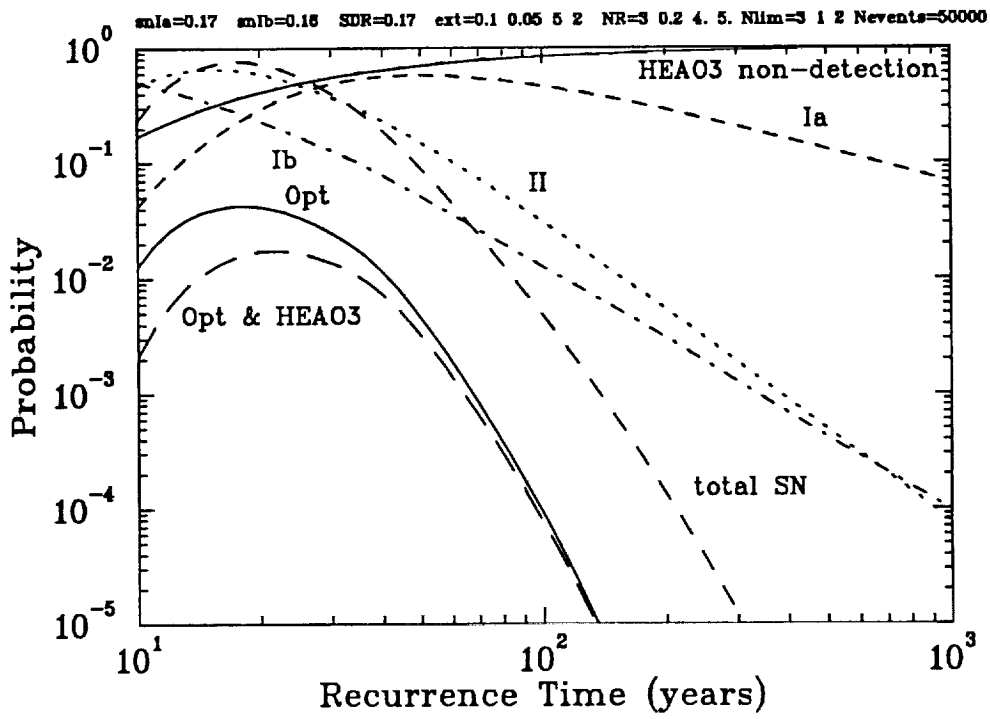

Figure 2: *Optical and γ-ray probabilities using the HEAO 3 flux limit.*

given location on the sky whose flux is modulated by the time dependent instrument response. Hypothetical point sources were assumed to be spaced 10° apart in Galactic longitude to assure maximum instrumental sensitivity. None of the resulting 36 bins along the Galactic plane showed any significant flux enhancement. HEAO 3 would have detected a source line flux of $\sim 2\times10^{-4}$ photons / cm^2 s about 99% of the time. This limit is used in this study.

Leising and Share (1991) have searched nearly ten years of data from NASA's Solar Maximum Mission (SMM) Gamma-Ray Spectrometer for evidence of γ-ray line emission from the decay of ^{44}Ti. They modeled the expected signals resulting from the annual scan of the ecliptic by SMM, considering point sources of various individual undiscovered events which might eject ^{44}Ti. They find no evidence of Galactic emission from ^{44}Ti, and find 99% confidence limits of 10^{-4} photons cm^{-2} s^{-1} for the 1.16 MeV line from ^{44}Sc from arbitrary points near the Galactic center. The limits on 1.16 MeV flux from longitudes near $\pm$ 90° rise to 2×10^{-4} cm^{-2} s^{-1} due to the reduced sensitivity in those directions.

Using the previously described procedures for randomly generating Galactic supernova events of all types, we perform a sufficient number of Monte Carlo simulations to determine the probabilities for detection of these events in the γ-ray band and the optical band. For a given average supernova rate in the Galaxy one can then analytically calculate the total probabilities for such histories to be consistent with the observed historic supernova record and the lack of γ-ray detections. Figure 2 shows a typical Monte Carlo result for a specific model of yields, extinction, relative SN frequencies, etc. The full curve "Opt" gives the probability that a history satisfies simultaneously the historic limits of each supernova type (i.e., 1-2 Ia; 2-4 Ib; 3-6 II). Individual probabilities are also shown. The dashed curve "total SN" gives the

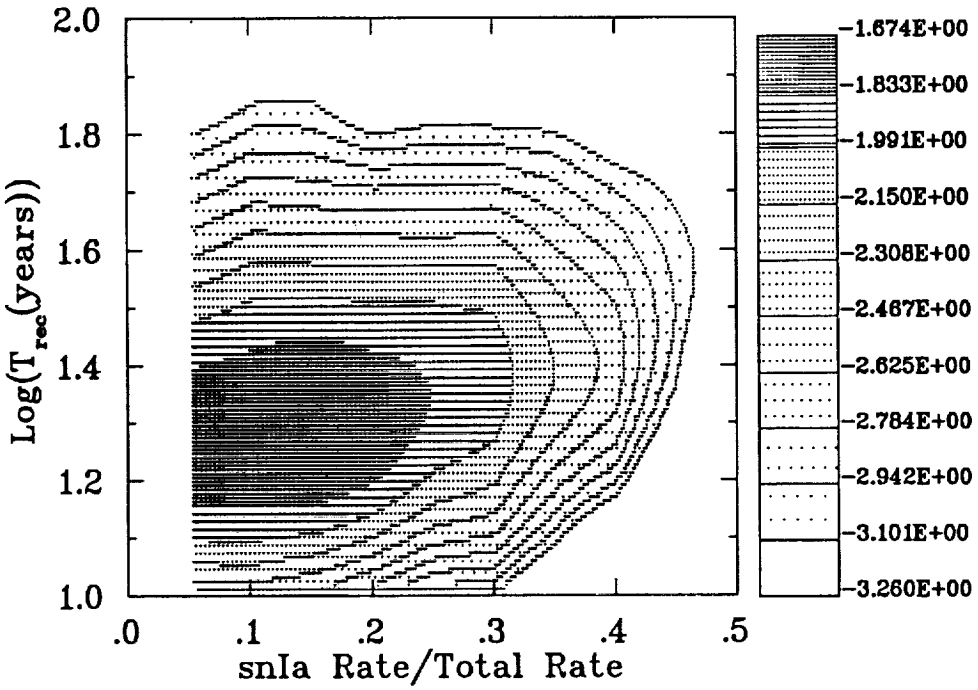

Figure 3: *Contours of combined optical and γ-ray probabilities as a function of total supernova rate and ratio Ia/(Ia+Ib+II). The labels give the logarithm of the joint probability for model histories to match the supernova record and to avoid HEAO 3 γ-ray detection.*

probability for the total number of SNe to be within the historic range (6-12), independent of type. The upper solid curve gives the probability for non-detection of γ-rays using the HEAO-3 limit. The lower dashed curve ("Opt&HEAO3") is the total combined probability for a model to satisfy both optical and γ-ray constraints. Based on optical data alone, the particular model shown in Figure 2 has a most likely supernova recurrence time of $\sim$ 18 years and the observed Galactic historic record is reproduced in about 4% of all Monte Carlo histories (this is still an acceptable model for Galactic supernova histories). Recurrence rates as short as 10 years yield only a 7% probability for non-detection of ^{44}Ti γ-ray lines. The combined optical/γ-ray model is thus severely constrained on the high frequency side, resulting in a most likely recurrence time of $\sim$ 23 years with peak probability to match both data sets of 1%. This model is thus still acceptable. Varying the total supernova rate and the ratio Ia/(Ia+Ib+II), we perform Monte Carlo simulations to determine the extent of the acceptable parameter space in which the combined probabilities exceed, say, 1%. The results (Figure 3) are fully consistent with those derived from extragalactic supernova searches, but we emphasize that γ-ray constraints on the recurrence times clearly rule out supernova frequencies as high as 1/10 years.

A detailed paper on these simulations is in preparation. This research was supported in part by NASA grants NAG 5-1578 and NAGW-2525, NSF grants 8813649 and 9115367, and grants SF-ENG-48 and W-7405-ENG-48.

REFERENCES

Adelberger, D. C. & Harbottle, G. 1990, Phys. Rev. C, 41, 2320

Branch, D. 1990, in *Supernovae*, ed. S. Bludman, R. Mochkovitch & J. Zinn-Justin, in press

Branch, D. & Tammann, G. A. 1991, ARA&A, in press

Burstein, D., & Heiles, C. 1978, ApJ, 225, 40

Burstein, D., & McDonald L. H. 1975, AJ, 80, 17

Ciardullo, R., Ford, H. C., Neill, J. D., Jacoby, G. H., & Shafter, A. W. 1987, ApJ, 318, 520

Disney, M., Davies, J., and Phillips, S. 1989, MNRAS, 239, 939

Evans, R., van den Bergh, S., & McClure, R. D. 1989, ApJ, 345, 752

Frekers, D., *et al.* 1983, Phys. Rev. C, 28, 1756

Hashimoto, M., Nomoto, K., & Shigeyama, T. 1989, A&A, 210, L5

Heiles, C. 1976, ApJ, 204, 379

Higdon, J. C., & Fowler, W. A. 1987, ApJ, 317, 710

Kumagai, S., *et al.* 1989, ApJ, 345, 412

Leibundgut, B. 1991, in *Supernovae*, ed. S. E. Woosley, (Springer: Heidelberg), 751

Leibundgut, B. & Tammann, G. A. 1990, A&A, 230, 81

Leising, M. & Share, G. 1991, ApJ, in preparation

Mahoney, W. A., Ling, J. C., Wheaton, W. A., & Higdon, J. C. 1991, in *Gamma-Ray Line Astrophysics*, ed. P. Durouchoux & N. Prantzos, (AIP: New York), 291

Mihalas, D. & Binney, J. 1981, *Galactic Astronomy*, (Freeman: San Fransisco).

Porter, A. C. & Filipenko, A. V. 1987, AJ, 93, 1372

Ratnatunga, K. U. & van den Bergh, S. 1989, ApJ, 343, 713

Sandage, A., & Tammann, G. 1981, *Revised Shapley Ames Catalog of Bright Galaxies*, Carnagie Institute, Washington

Schmitz, M. R. & Gaskell, C. M. 1988, in *Supernova 1987A in the Large Magellanic Cloud*, ed. M. Kafatos & A. G. Michalitsianos, (Cambridge Univ. Press: Cambridge), 112

Suntzeff, N. B., Phillips, M. M., Depoy, D. L., Elias, J. H., & Walker, A. R. 1991, AJ, 102, 1118

Tammann, G. & Schröder, A. 1990, A&A, 236, 149

Tammann, G. A. 1991, in *Supernovae*, ed. S. Bludman, R. Mochkovitch, and J. Zinn-Justin, (Elsevier Sci. Publ.), in press

Valentijn, E. A. 1991, Nature, 346, 153

van den Bergh, S. 1990, AJ, 99, 843

van den Bergh, S. 1991a, in *Supernovae*, ed. S. E. Woosley, (Springer: Heidelberg), 711

van den Bergh, S. 1991b, *Phys. Rep.*, in press

van den Bergh, S. & Tammann, G. A. 1991, ARA&A, 29, 363

Woosley, S. E., Arnett, W. D., & Clayton, D. D. 1973, ApJS, 175, 731

Woosley, S. E. 1986, in *Nucleosynthesis and Chemical Evolution*, 16th Adv. Course of the Swiss Soc. of A&A, ed. B. Hauck, A. Maeder, and G. Meynet, (Geneva Obs.: Geneva), 1

Woosley, S. E. 1991, in *Gamma-Ray Line Astrophysics*, ed. P. Durouchoux & N. Prantzos, (AIP: New York), 270

Woosley, S. E & Pinto, P. 1988, in *Nuclear Spectroscopy of Astrophysical Sources*, ed. N. Gehrels & G. Share, (AIP: Washington DC), AIP 170, 98

Woosley, S. E., & Hoffman, R. D. 1991, ApJL, 368, L31 (WH)

Woosley, S. E., Pinto, P., & Weaver, T. A. 1988, *Proc. Astr. Soc. Australia*, 7, No. 4, 355

Woosley, S. E., Pinto, P., & Hartmann, D. 1989, ApJ, 346, 395

Gamma Ray Pulsar Analysis from Photon Probability Maps

Lawrence E. Brown, Donald D. Clayton, and Dieter H. Hartmann
Department of Physics and Astronomy
Clemson University
Clemson, SC 29634-1911, U.S.A.

Abstract

We present a new method of analyzing skymap-type γ-ray data. Each photon event is replaced by a probability distribution on the sky corresponding to the observing instrument's point spread function. The skymap produced by this process may be useful for source detection or identification. Most important, the use of these photon weights for pulsar analysis promises significant improvement over traditional techniques.

1 The Method

We have used the derived point spread function for the COS-B experiment to develop data analysis tools with improved ratios of signal to background with applications to source identification and searches for faint γ-ray pulsars. We generate a weighted photon probability map to enhance any significant γ-ray signal present in the data and suppress undesirable background fluctuations. The basis for this method can be formulated in two equivalent ways:

a) By definition, the point spread function (PSF) of an imaging instrument describes the redistribution of photons from a particular direction on the sky into the observed distribution. Thus, each event may be represented as a continuous distribution of event weights on the sky (for COS-B, the PSF vanishes for $\theta > 20°$).

b) Correspondingly, any location on the sky recieves some weight from each γ-ray seen during the experiment. In other words, each observed photon has a certain probability, given by the PSF, to have originated at that location.

Based on this concept, we smooth each photon arrival direction into an extended probability map. When investigating a particular source location, our analysis includes *all* γ-ray events through their weights at that position. To demonstrate the usefulness of this approach we apply it to the light curve of the Crab pulsar. The extraction of a source list from our COS-B probability map is in progress.

2 COS-B Probability Maps

The observed direction of each photon event does not correspond directly to its point of origin on the sky. Information on the detector angular resolution is contained in the PSF of the detector. To identify γ-ray ray sources, the intrinsic fuzziness of γ-ray detectors can be included in the analysis by creating a skymap of "probability flux" rather than "photon count flux".

The weight of a γ-ray event with observed direction α for a small solid angle $\Delta\theta$ centered on a point p is defined as

$$w(p;\alpha) = PSFSR(\theta(\alpha,p))\Delta\theta,$$

where PSFSR is the point spread function per steradian. We use the PSFSR derived by the COS-B team using the Vela pulsar (Mayer-Hasselwander 1985).

The celestial γ-ray intensity, I_c, at a point on the sky (in terms of weight) is

$$I_c(p) = \frac{\Sigma_{\gamma's} w(p) - \int_{sky} d\Omega w(\Delta N_b(p))}{\int_{sky} d\Omega w(\Pi(p))} - I_b,$$

where the summations are taken over all events seen by the experiment, the $w(p)$'s are the weights of the individual events, $w(\Delta N_b(p))$ is the weight, at p, of the instrumental background correction for all other points on the sky, and $w(\Pi(p))$ is the weight, at p, of the exposure (in $cm^2\ s$) for all other points on the sky. I_b is the "standard" background correction as given by the COS-B team. The units of I_c are $photons/cm^2\ s\ sr$.

This defines our weighted sky intensity probability distribution. We have sampled this continuous map at .5° intervals for the whole sky. The resultant maps in the energy ranges 50-150 MeV, 150-300 MeV, and 300-5,000 MeV are shown in figure 1.

This technique may not be ideal for some aspects of *source identification.* It results in a skymap which may be "too fuzzy" since the photons are effectively convolved twice through the PSF. That is, they are spread once in passing through the detector and again by our technique. However, it does not make any arbitrary smoothing assumptions. A comparison of our source list (in progress) with those resulting from other techniques (e. g.Simpson & Mayer-Hasselwander 1987; Bloemen 1989) will be useful. For instance, our technique finds a possible source of high intensity but low statistical weight at $l = 309.5, b = -30.5$ in the middle energy range (see figure) it should be instructive to see if the maximum likelihood methods of Grenier, et al. confirm this source candidate.

3 Lightcurve of the Crab Pulsar

For analysis of periodic sources, we analyze weights vs. phase instead of counts vs. phase. Superimposed on a background that is $\sim$ uniform in space and time, the γ-ray pulsar adds a signal that is localized both in space and time. Standard analysis of γ-ray phases considers all photons within a given acceptance cone equally. Photon arrival directions

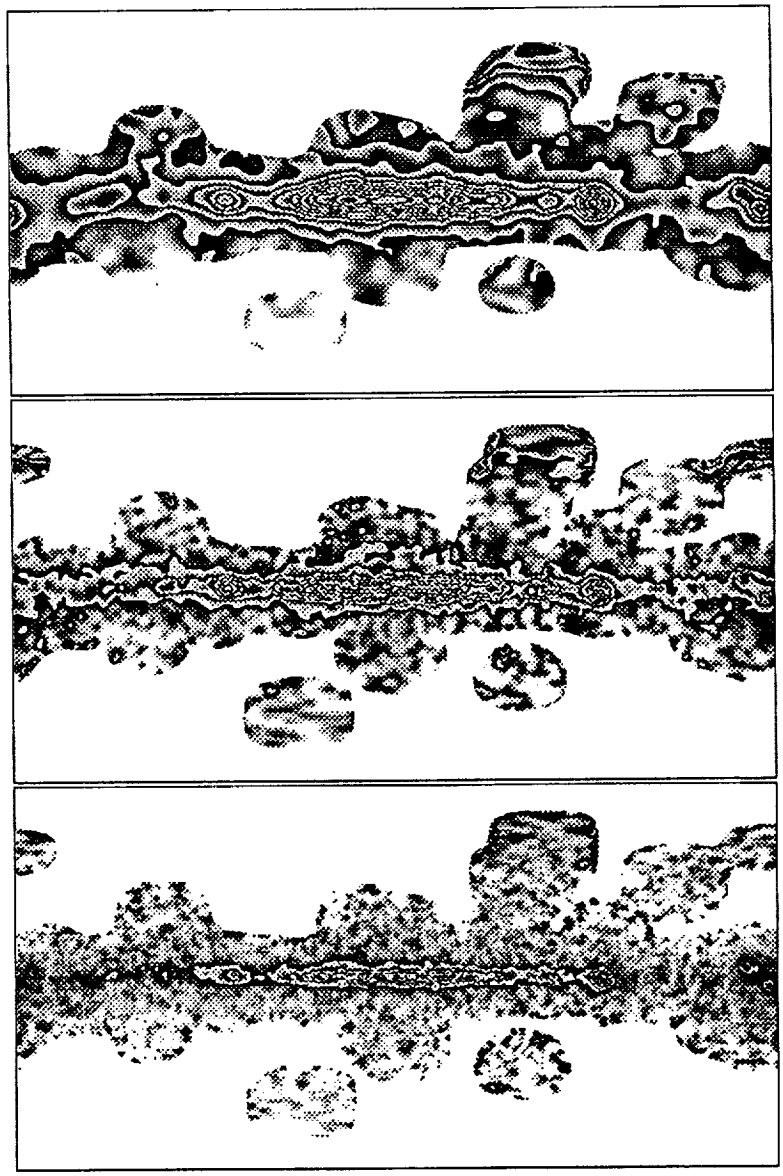

Figure 1: *Skymaps of photon weight of the COS-B observations for the energy ranges 50-150 MeV, 150-300 MeV, and 300-5,000 MeV. The photon weight distribution on the whole sky is sampled on a grid of .5 degree spacing. Since COS-B did not observe all areas of the sky, some regions of the map at high galactic latitudes are blank. The graymaps used here represent intensity of* photons/cm^2 s sr, *with intensity increasing from black to white. This graymap is wrapped around 10 times between the faintest and brightest spots for better monochrome resolution. It is, essentially a grayscale "contour map". The graymaps are assigned individually for each map (i. e. equal gray intensities on different maps do not represent equal photon fluxes).*

TABLE 1: Signal to background

Observation	Peak Signal (Std. Dev.)		Integrated Signal (Std. Dev.)	
	weights	counts	weights	counts
Crab Pulsar	43	18	176	101
1/2 Crab Pulsar	33	12	107	59

closer to the pulsar position have a higher probability of containing the sought after pulsed signal. Thus, by considering both space and time, we gain an added degree of freedom for extracting the signal from the background.

The standard binning technique folds solar barycentric arrival times with the measured period characteristics obtained from radio observations (Buccheri, et al. 1983). Traditionally, one defines an acceptance cone around the source direction with opening angle

$$\theta_{max} = 12.5E(MeV)^{-.16}.$$

Inside this cone, all photons contribute equally to the light curve. In our approach, PSF weighting implicitly performs this task; thus, we can utilize the maximum aperture consistent with a non-zero PSF ($\theta_{max} = 20°$ for COS-B).

Then, instead of binning counts by phase to create a light curve histogram, we bin weights by phase. Results for the two methods for the Crab Pulsar are shown in our figure 2.

Figure 3 highlights the differences between the two approaches. Essentially, the traditional method uses a uniform probability function inside an acceptance cone that has an energy dependent width. We have used, instead, a probability function which extends over the full range of non-zero PSF, but binned into 3 energy ranges. This binning follows COS-B tradition, could easily be made finer.

To allow direct comparison of the two methods, we plot the standard deviation for each bin. To calculate the average background level, we have used the "flat" portion of the Crab pulsar's γ-ray light curve between the second peak and the end of the period. The resulting plot shows counts (weights) minus average background divided by standard deviation from background. We show results for all, and half of the Crab pulsar observations of COS-B to demonstrate the performance of this technique for reduced sampling times. The results in terms of maximum signal above background and total integrated signal are given in table 1. While the exact numbers are dependent on bin size, the improvement is dramatic in all cases.

This obvious increase in significance of detected pulses should also benefit the cluster analysis algorithm of Buccheri, et al. (1988). We are currently investigating this and other extensions to the general weighting technique.

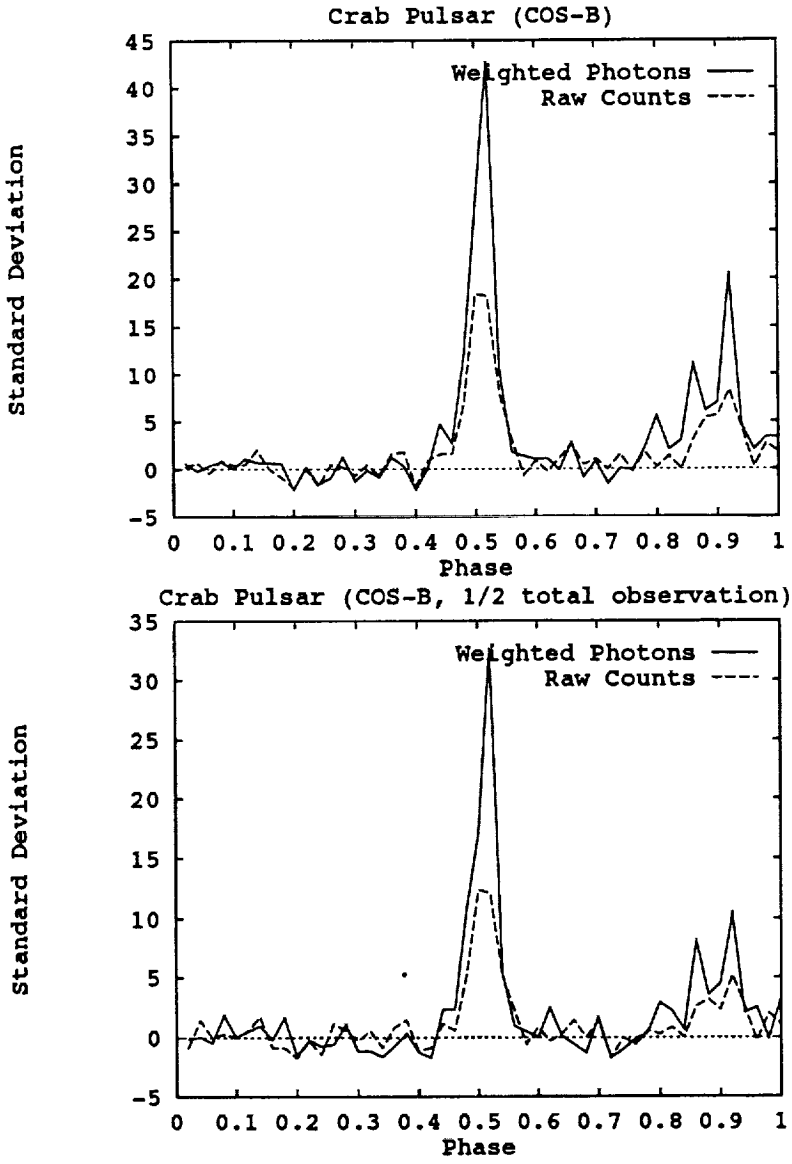

Figure 2: *Shown are the weighted photon method (solid) and the standard count method (dashed) of phase binning for the full COS-B data set for the Crab pulsar. Note the dramatically improved signal for the weighted photon method. (Number of bins = 50.)*

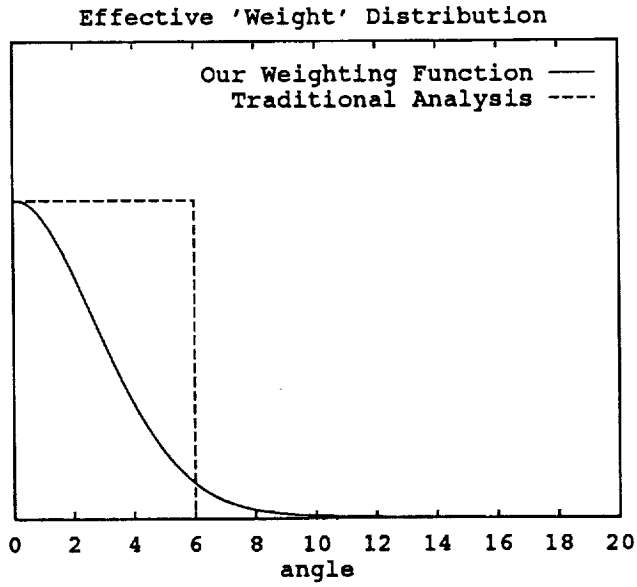

Figure 3: *Schematic drawing comparing the effective probability "weight" distribution for traditional pulsar analysis (dashed) and our weighting function (solid) for a given energy* ($\sim 100 MeV$).

Acknowledgements

This research was supported in part by NASA Grant NAG 5-1578. We thank Mark Leising and Lih-Sin The for many valuable discussions.

References

Bloemen, H. 1989, *Ann. Rev. Astron. Astrophys.*, **27**, 469

Buccheri, R., et al. 1983, *Astron. Astrophys.*, **128**,245

Buccheri, R., Di Gesu', V., Maccarone, M.C., and Sacco, B. 1988, *Astron. Astrophys.*, **201**,194

Grenier, I.A., Hermsen, W., and Pollock, A.M.T. 1991, in *AIP Conference Proceedings*, (New York), p. 3.

Mayer-Hasselwander, H. A. , ed. 1985, *Explanatory Supplement to the COS-B Final Database.*

Simpson, G., and Mayer-Hasselwander, H.A. 1987, *Proceedings of the 20th ICRC*, (Moscow), 1:89